ELSEVIER

Cardiovascular Research 64 (2004) 365–373

Cardiovascular Research

www.elsevier.com/locate/cardiores

# Cardiac outflow tract malformations in chick embryos exposed to homocysteine

Marit J. Boot[a], Régine P.M. Steegers-Theunissen[b,c], Robert E. Poelmann[a], Liesbeth van Iperen[a], Adriana C. Gittenberger-de Groot[a,*]

[a]*Department of Anatomy and Embryology, Leiden University Medical Center, PO Box 9602, 2300 RC Leiden, The Netherlands*
[b]*Department of Obstetrics and Gynaecology, Erasmus Medical Center Rotterdam, The Netherlands*
[c]*Department of Epidemiology and Biostatistics, University Medical Center Nijmegen, The Netherlands*

Received 2 March 2004; received in revised form 17 June 2004; accepted 16 July 2004
Available online 14 August 2004
**Time for primary review 27 days**

**Abstract**

**Objective:** Increased homocysteine concentrations have been associated with cardiac outflow tract defects. It has been hypothesized that cardiac neural crest cells were the target cells in these malformations. Cardiac neural crest cells migrate from the neural tube and contribute to the condensed mesenchyme of the aorticopulmonary septum and outflow tract cushions of the heart. The aim of this study is to investigate the effects of homocysteine on cardiac neural crest cells in relation to heart malformations.
**Methods:** Homocysteine was injected either into the neural tube lumen (30 μmol/l), or into the circulatory system (30 or 300 μmol/l) of chick embryos. *LacZ*-retroviral labeling was used to study cardiac neural crest cell migratory pathways after exposure to homocysteine.
**Results:** Cardiac neural crest cells contributed to the aorticopulmonary septum of both control and homocysteine-treated embryos. However, the outflow tract of homocysteine-neural tube injected embryos displayed 60% less apoptosis and 25% reduced myocardialization. A subarterial ventricular septal defect was observed in 83% of the embryos. None of these abnormalities were observed in homcysteine-circulatory system injected embryos.
**Conclusion:** This study demonstrates that homocysteine disturbs apoptosis and myocardialization of the outflow tract, probably by affecting the cardiac neural crest cells.


*Keywords:* Apoptosis; Congenital defects; Developmental biology

## 1. Introduction

Periconceptional use of folic acid or multivitamins containing folic acid reduce the risk of neural tube defects [1,2] and conotruncal heart defects [3,4] in the offspring. Folate is involved in the remethylation of homocysteine into methionine, therefore a low folate status can result in an accumulation of homocysteine [5]. Mildly elevated levels of homocysteine in maternal blood and amniotic fluid have been associated with neural tube defects [6,7] and congenital heart defects [8]. This is in line with an in vivo study in which high concentrations of homocysteine administered on top of chick embryos resulted in neural tube defects, orofacial malformations, conotruncal heart defects, and ventral midline defects in a time- and concentration-dependent manner [9]. Although the involvement of cardiac neural crest cells was suggested, no evidence was given to support this theory.

Cardiac neural crest cells are formed at the fusion site of the neural folds when the folds give rise to the neural tube.

*Abbreviations:* Ao, ascending aorta (light red); P, pulmonary trunk (light green); LV, left ventricle (dark red); NT, homocysteine-neural tube injected; RV, right ventricle (dark green)

* Corresponding author. Tel.: +31 71 5276660; fax:+31 71 5276680.
*E-mail address:* A.C.Gittenberger-de_Groot@lumc.nl (A.C. Gittenberger-de Groot).

0008-6363/$ - see front matter © 2004 European Society of Cardiology. Published by Elsevier B.V. All rights reserved.
doi:10.1016/j.cardiores.2004.07.010

The cardiac neural crest cells are derived from the neural tube region between the otic placode and the caudal limit of somite 3 [10]. Cardiac neural crest cells were shown to contribute to the condensed mesenchyme and prongs of the aorticopulmonary septum, the outflow tract cushions, the smooth muscle layers of the pharyngeal arch arteries, and the cardiac ganglia, by using quail-chick chimeras [11,12] and retroviral labeling [13,14].

In vitro studies have demonstrated that high homocysteine concentrations increase neural crest cell motility and migration distance [15], as well as the neural crest cell outgrowth area, but decreased the neural crest cell differentiation into smooth muscle cells and nerve cells. However, homocysteine did not seem to affect the low numbers of apoptotic cells that are observed in neural crest cultures [16]. The aim of this study is to analyze the effects of homocysteine on neural crest cells and their role in cardiogenesis at the developmental stage when neural crest migration has just started. Furthermore, homocysteine-circulatory system injections were performed at the first stage when the circulatory system is a closed circuit, the pharyngeal arch artery system is just established, and the endothelial cells are not yet surrounded by differentiated neural crest cells. With these experiments we studied if there are differences between local exposure to homocysteine (pre-migratory neural crest in the neural folds) and general exposure to homocysteine (circulatory system). The first part of this study focuses on the effects of homocysteine on cardiac neural crest cell migration pathways and the expression of the neural crest related gene *Pax3*. An association between *Pax3* and folic acid has been suggested, while folic acid had a protective effect against neural tube defects in *Pax3*-deficient *Splotch* mice [17]. The second part describes the homing of neural crest cells and the apoptosis patterns in the cardiac outflow tract after homocysteine exposure. The third part demonstrates the effects of homocysteine on outflow tract cushion fusion, the development of subarterial ventricular septal defects (VSD), and the myocardialization of the outflow tract cushions.

## 2. Materials and methods

### 2.1. Injection of homocysteine into chick embryos

For neural tube experiments, fertilized specified pathogen free White Leghorn eggs were incubated at 37 °C for 33–40 h and subsequently windowed at Hamburger and Hamilton [18] stages 9–10. Neural crest cell tracing studies were performed on chick embryos using a replication-incompetent spleen-necrosis retrovirus with a *lacZ* gene [19,20]. The retrovirus solution in M199 medium was mixed with polybrene (100 μg/ml) to increase transduction, and indigo carmine blue (0.25 g/ml) for visualization. Combined solutions of retrovirus and L-homocysteine thiolactone hydrochloride (30 μmol/l) were used to study the effect of homocysteine on *lacZ*-marked neural crest cell migration. The effect of homocysteine on *Pax3* expression and heart development was studied using a solution of L-homocysteine thioloactone hydrochloride (30 μmol/l) and indigo carmine blue (0.25 g/ml) in M199 medium. Injections were made into the neural tube lumen at somite levels 4–6, filling the neural tube in anterior direction until the solution reached the otic placode level as described before [20]. These embryos were called the NT group.

For circulatory system experiments, eggs were incubated at 37°C for 54–56 h and windowed at HH14. L-Homocysteine thioloactone hydrochloride (30 μmol/l or 300 μmol/l), indigo carmine blue (0.25 g/ml) in M199 medium, was injected into the marginal sinus of the yolk sac vasculature. Within 3 s, 1/8 of the yolk sac vasculature and the intra-embryonic circulatory system was filled with the homocysteine solution as justified by the spreading of the indigo carmine blue coloring. The homocysteine solution quickly mixed with the blood present in the circulatory system, and was therefore diluted approximately 8 times. The embryos that received a homocysteine solution into the circulatory system were called CS embryos. Following injection, the eggs were sealed with Scotch tape and returned to the incubator for further development.

### 2.2. Tissue preparation, β-galactosidase staining, and immunohistochemistry

One embryo of the NT group showed a ventral midline defect at HH35 and was therefore excluded from this study.

The following number of embryos was analyzed—NT: HH18–19 ($n$=8), HH30–31 ($n$=9), HH35 ($n$=6); CS (30 μmol/l): HH30–31 ($n$=2), HH35 ($n$=4); CS (300 μmol/l): HH30–31 ($n$=8), HH35 ($n$=3); control embryos: HH18–19 ($n$=8), HH30–31 ($n$=12), HH35 ($n$=8).

The *lacZ*-retrovirus injected embryos were immersion fixed in toto in 2% paraformaldehyde in 0.1 mol/l phosphate buffer for 1 h. Extensive rinsing of the embryos in PBS was followed by immersion in X-gal solution (PBS containing 5 mmol/l potassium ferricyanide, 5 mmol/l potassium ferrocyanide, 2 mmol/l $MgCl_2$ and X-Gal (5-bromo-4-chloro-3 indolyl β-D-galactopyranoside) for 2–5 h at 37 °C to stain for the presence of β-galactosidase.

The HH35 embryos were first perfused with 4% paraformaldehyde in 0.1 mol/l phosphate buffer through the liver, subsequently the thorax was isolated and immersion fixed overnight. The tissues were dehydrated in graded ethanol and embedded in paraffin.

Serial sections (5 μm) were cut and sequentially distributed over glass slides. The alternate sections were incubated overnight with HHF35 (diluted 1:1000, anti-

muscle specific actins; Dako Denmark), JB3 (diluted 1:2, anti-fibrillin-2, a gift from Dr. R.R. Markwald, Charleston, USA), MF20 (diluted 1:5, anti-myosin heavy chain, Hybridomabank, Iowa City, USA) as described before [20,21]. Additionally, sections were microwave-processed to enhance JB3 and MF20 staining. Sections were stained for apoptotic cells using the TUNEL procedure (Boehringer, Mannheim, Germany), as previously described [13], however, the sections were not pretreated with proteinaseK and were incubated in TUNEL mix for 90 min. After the DAB procedure, sections were briefly counterstained with Mayer's hematoxylin, dehydrated and mounted in Entellan. Adjacent sections were stained for 5 min with hematoxylin and analyzed for cell death as described previously [22].

### 2.3. Pax-3 in situ hybridization

A 660-bp chick Pax3 probe (kindly provided by P. Gruss, Max Planck Institute, Göttingen, Germany) was used for non-radioactive in situ hybridization on 14-μm paraffin sections using the NBT/BCIP chromogenic substrate as described by Moorman and coworkers [23], with the adaptation that the hybridization temperature was set at 65 °C and no tyramide signal amplification step was used.

### 2.4. TUNEL analysis, outflow tract cushion volume estimations, and 3D reconstructions

The number of TUNEL positive cells in the outflow tract was counted in every 7th section. For the TUNEL analysis 8 control embryos (HH30 $n$=2; HH31 $n$=6) and 8 NT embryos (HH30 $n$=3; HH31 $n$=5) were used. The results were statistically analyzed using the Mann–Whitney test for independent groups and the results are presented per group as the median of the number of observed apoptotic cells and the inter-quartile range (IQR), showing the variation within the groups.

The volume of the outflow tract cushions that was not populated by myocardial cells was estimated in actin-stained sections of HH35 embryos using the Cavalieri technique [24], as described before for the outflow tract cushion volume [25]. We analyzed every 7th section along the complete length of the outflow tract cushions of five control embryos, five CS embryos, and five NT embryos. The volume measurements were statistically analyzed using the Mann–Whitney test for independent groups. The results are presented as the median with the inter-quartile range.

Three-dimensional reconstructions of serially sectioned hearts were made using Amira 3.0 software. For both the control and the NT group 3 lumen reconstructions were made, the variation within the group was small, therefore the lumen reconstructions shown here are representative of the group.

## 3. Results

### 3.1. Cardiac neural crest cell migration pathways and Pax3 expression in homocysteine-neural tube injected (NT) embryos

Embryos were injected into the neural tube lumen with either a solution of *lacZ*-retrovirus or a combined solution of homocysteine and *lacZ*-retrovirus. The *lacZ*-retrovirus can integrate in the genome of replicating cells lining the neural tube lumen. Therefore, neural crest cells that were transduced with the *lacZ*-retrovirus stain blue for the β-galactosidase product and can be traced in all stages of their migration to the heart, providing a basis for their distribution pattern in the embryo. In addition to neural crest cells, the neuroepithelial cells of the neural tube are transduced, however in a previous study we demonstrated that only the neural crest cells from the dorsal side can migrate from the neural tube and no ventral emigrating cells exist [20]. Furthermore, if careful injections are made no other tissues are labeled by the retroviral injection, with the exception of occasional ectoderm cells [13].

At HH18, *lacZ*-positive cardiac neural crest cells were observed in the mesenchyme of the pharyngeal arches surrounding the pharyngeal arch arteries in both control embryos (Fig. 1a) and homocysteine-neural tube injected (NT) embryos (Fig. 1e). The leading edge of the *lacZ*-positive cardiac neural crest cells was located in the aortic sac region in control embryos (Fig. 1b), as well as in NT embryos (Fig. 1f). At HH18 *Pax3* mRNA expression was analyzed and observed at the dorsal side of the neural tube, in the dorsal root ganglia, as well as in the dorsolateral stream of neural crest cells in both control (Fig. 1c) and NT embryos (Fig. 1g). We did not observe any differences in the distribution pattern of *lacZ*-positive neural crest cells or *Pax3* expression between control and NT embryos at HH18.

In embryos (HH18), the heart tube consisted of an endocardial and a myocardial layer separated by cardiac jelly. In control embryos, the cardiac jelly at the level of the outflow tract contained groups of mesenchymal cells and was rich in dispersed fibrillin-2-positive fibers (Fig. 1d). The NT embryos, however, only displayed subendothelial fibrillin-2 protein expression and a low number of mesenchymal cells in the cardiac jelly at the level of the outflow tract (Fig. 1h). Scattered fibrillin-2 fibers were observed in the cardiac jelly of the atrioventricular (AV) cushions in both control and NT embryos (not shown).

### 3.2. Cardiac neural crest cell homing and apoptosis in the outflow tract of NT embryos

At HH31, *lacZ*-positive cardiac neural crest cells were observed in the vessel walls of the third, fourth and sixth pharyngeal arch arteries and in the condensed mesenchyme of the outflow tract in both control (Fig. 2a) and NT

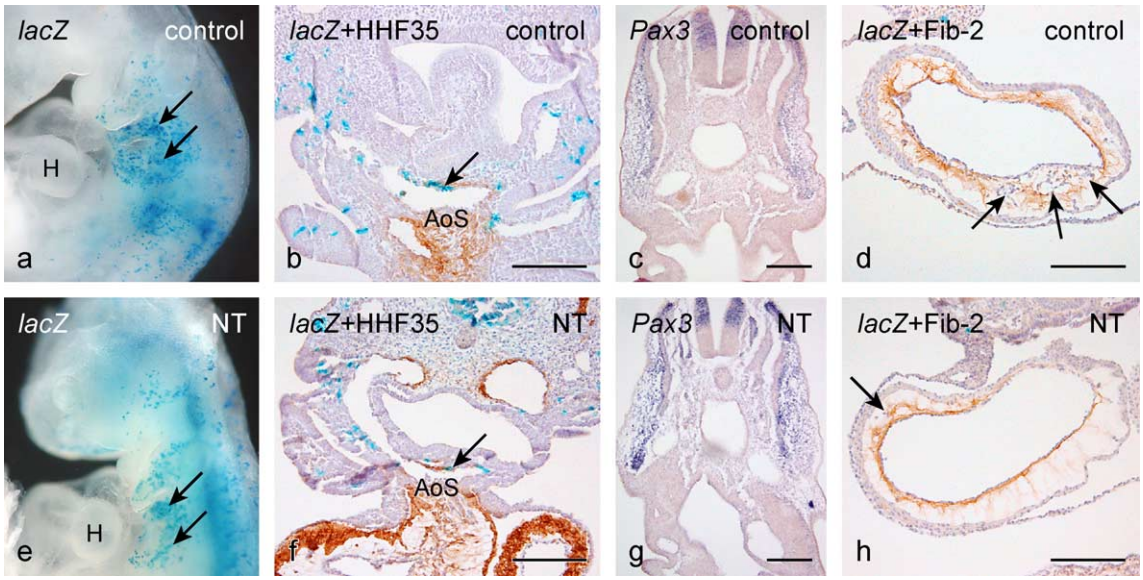


Fig. 1. HH18–19 control and homocysteine-neural tube injected embryos. (a, b, d) HH18 control embryo injected with *lacZ*-retrovirus. (a) *LacZ*-positive neural crest cells in the pharyngeal arches (arrows). (b) Transverse section shows the *lacZ*-positive cells in the pharyngeal arches and the aortic sac (AoS) region (arrow), the brown staining (HHF35) shows the actin positive cells of the aortic sac. (c) Transverse section of HH19 control embryo with *Pax3* expression in dorsal part of neural tube and dorsolateral neural crest pathway. (d) Transverse section of HH18 outflow tract with dispersed fibrillin-2 (Fib-2) expression and mesenchymal cells (arrows) in the cardiac jelly. (e, f, h) HH18 NT embryo. (e) *LacZ*-positive neural crest cells in the pharyngeal arches (arrows). (f) Transverse section shows *lacZ*-positive cells in the pharyngeal arches and the aortic sac (AoS) region (arrow). (g) Transverse section of HH19 NT embryo. *Pax3* expression is located in similar positions as in the control embryo: the dorsal part of the neural tube, dorsal root ganglia and dorsolateral neural crest pathway. (h) Transverse section of HH18 outflow tract with subendothelial fibrillin-2 expression and only a few mesenchymal cells (arrow) in the cardiac jelly. H, heart; NT, homocysteine-neural tube injected. Bar=150 μm.

embryos (Fig. 2d). The roots of the ascending aorta and pulmonary trunk were separated by the aorticopulmonary septum in both control and NT embryos. At semilunar valve level myocardialization of the outflow tract had started and myocardial cells were observed in the mesenchymal area centrally between the aortic and pulmonary valves. Myocardialization was obvious in control embryos (Fig. 2b), however, myocardialization was almost absent in NT embryos (Fig. 2e). In the NT embryos the myocardial cells remained at the periphery along the complete length of the outflow tract.

In control embryos, the area containing myocardial cells was rich in TUNEL-positive cells (Fig. 2c). In NT embryos the area containing myocardial cells displayed only a few TUNEL-positive cells, and only a few TUNEL-positive cells were observed in the outflow tract cushions and pulmonary valves (Fig. 2f). By analyzing an adjacent section stained for muscle actin (HHF35) we noticed that most apoptotic cells were located adjacent to myocardial cells, however some TUNEL positive cells were in a location that was actin positive in adjacent sections and were therefore presumably myocardial cells.

The observed number of TUNEL-positive cells in the outflow tract of control embryos was 186 (IQR 78), and in NT embryos 75 (IQR 74). The number of observed TUNEL-positive cells is 60% lower in NT embryos compared to control embryos, this is a significant ($p<0.01$) difference as demonstrated by statistical analysis with the Mann–Whitney test (Fig. 3). To confirm that the TUNEL positive cells represented apoptotic cells we studied the morphology of these cells by hematoxylin staining. As indicated with arrows (Fig. 2g) most cells that are positive for TUNEL in a section of the outflow tract were traced in an adjacent section and were demonstrated to have morphological characteristics typical for apoptosis like condensed and fractured nuclei and cell shrinkage.

### 3.3. Cushion fusion and myocardialization is affected in NT embryos

In control embryos (HH35), the outflow tract cushions were completely fused. The outflow tract cushions were invaded by a large number of myocardial cells as demonstrated by muscle actin (HHF35) staining and myosin heavy chain (MF-20) staining (Fig. 4a–c). The immunohistochemical staining with MF20 was comparable to the HHF35 staining in the outflow tract region.

In contrast to the complete cushion fusion observed in control embryos, 5 out of 6 NT embryos displayed an incomplete fusion of the outflow tract cushions, which resulted in subarterial VSD. The most distal borders of the VSDs involved either both pulmonary and aortic valves (Fig. 4d) or aortic valves and right ventricular outflow tract (Fig. 4e). Large parts of the outflow tract cushions in the embryos with subarterial VSDs were devoid of actin-positive myocardial cells (Fig. 4d–f), suggesting reduced myocardialization. The position and shape of the AV cushions in the NT embryos were similar to control

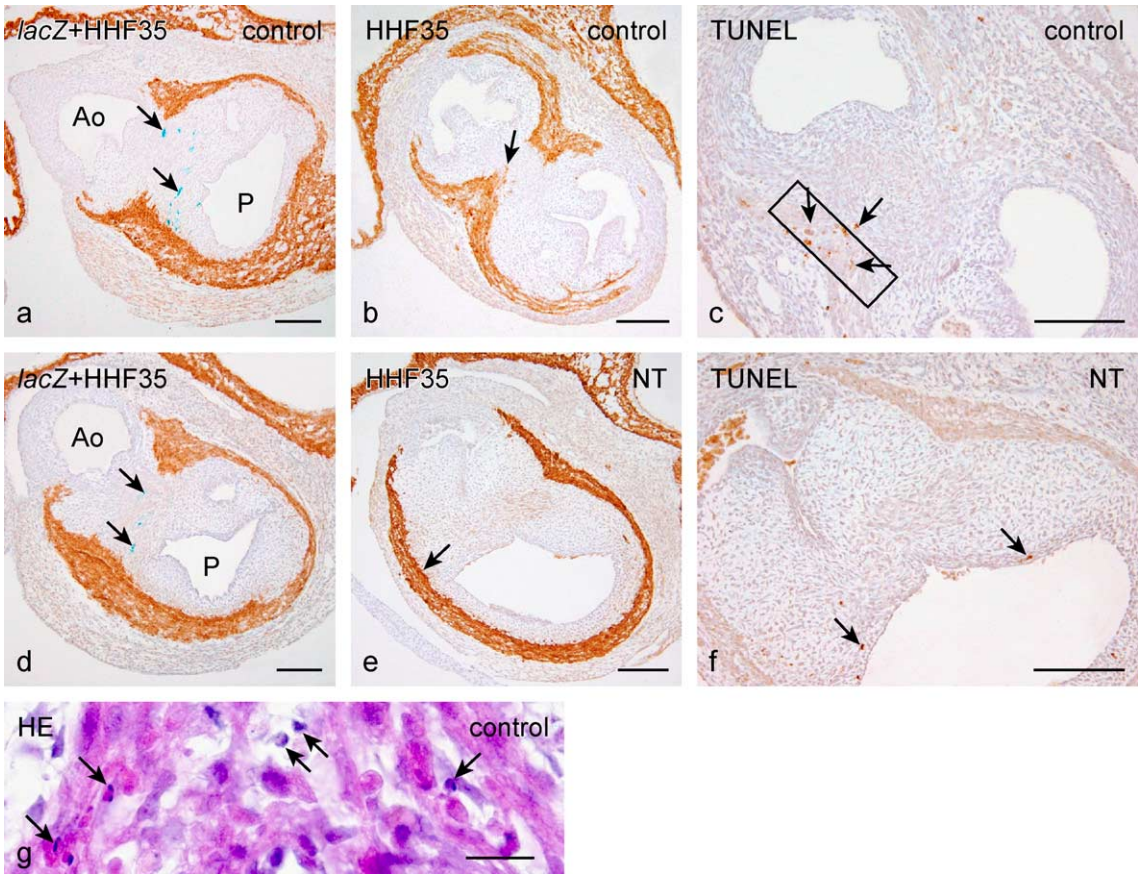


Fig. 2. Transverse sections of HH31 control and NT embryos. (a–c) Control embryos injected with *lacZ*-retrovirus. (a) *LacZ*-positive cells are observed in the aorticopulmonary septum between the ascending aorta (Ao) and pulmonary trunk (P) (arrows). (b) Actin (HHF35)-positive myocardial cells have invaded the condensed mesenchyme of the aorticopulmonary septum (arrow). (c) Adjacent section of (b), TUNEL-positive cells were predominantly observed in the area of invading myocardial cells (arrows). (d–f) Transverse sections of HH31 NT embryos. (d) *LacZ*-positive cells in the condensed mesenchyme (arrows) between the aortic and pulmonary valves. (e) Myocardial cells (arrow) are only located at the periphery of the outflow tract. (f) Adjacent section of e, TUNEL-positive cells are observed in the pulmonary valve leaflets (arrows). (g) Adjacent section of c, hematoxylin staining demonstrates a large number of apoptotic cells in the outflow tract area were myocardialization takes place. Many cells show an apoptotic morphology with condensed and fragmented nuclei (arrows). NT, homocysteine-neural tube injected. Bar (a–f): 150 μm, bar (g)=30 μm.

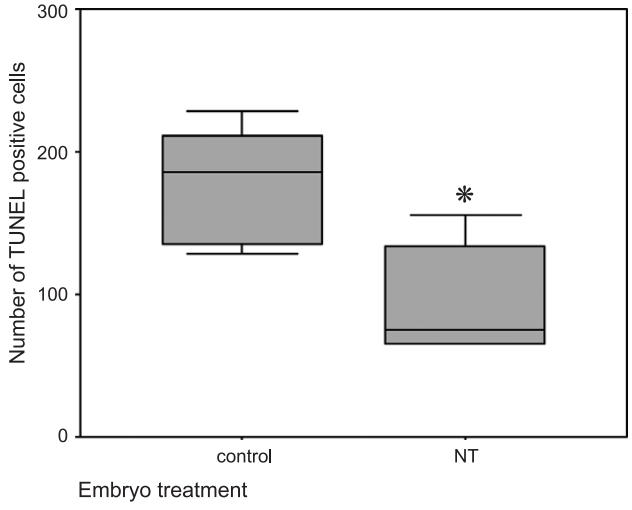


Fig. 3. Number of counted TUNEL positive cells in the outflow tract of control and homocysteine-neural tube injected (NT) embryos (HH30–31). The numbers of TUNEL positive cells are 60% lower in NT embryos compared to control embryos, which is significantly ($p<0.01$) lower as demonstrated with the Mann–Whitney test. *$p<0.01$.

embryos.The CS embryos that received a 30 or 300 μmol/l homocysteine injection into the circulatory system all showed normal fusion of the outflow tract cushions similar to control embryos (Fig. 4g, h). A large number of myocardial cells populated the area where the outflow tract cushions had fused (Fig. 4i), suggesting normal myocardialization.

The volume of the mesenchymal outflow tract cushion tissue that was not myocardialized, was estimated in embryos HH35 using the Cavalieri technique. The outflow tract cushion volume was 0.059 $mm^3$ (IQR 0.009) for control embryos, 0.060 $mm^3$ (IQR 0.006) for CS embryos, but as high as 0.074 $mm^3$ (IQR 0.006) for NT embryos (Fig. 5). The group of NT embryos showed a 25% larger volume of non-myocardialized outflow tract cushion tissue compared to control embryos, this is significant ($p<0.005$) as shown by statistical analysis. Also the embryo in the NT group with normally fused outflow tract cushions showed an increased volume (0.076 $mm^3$) of non-myocardialized cushion tissue.

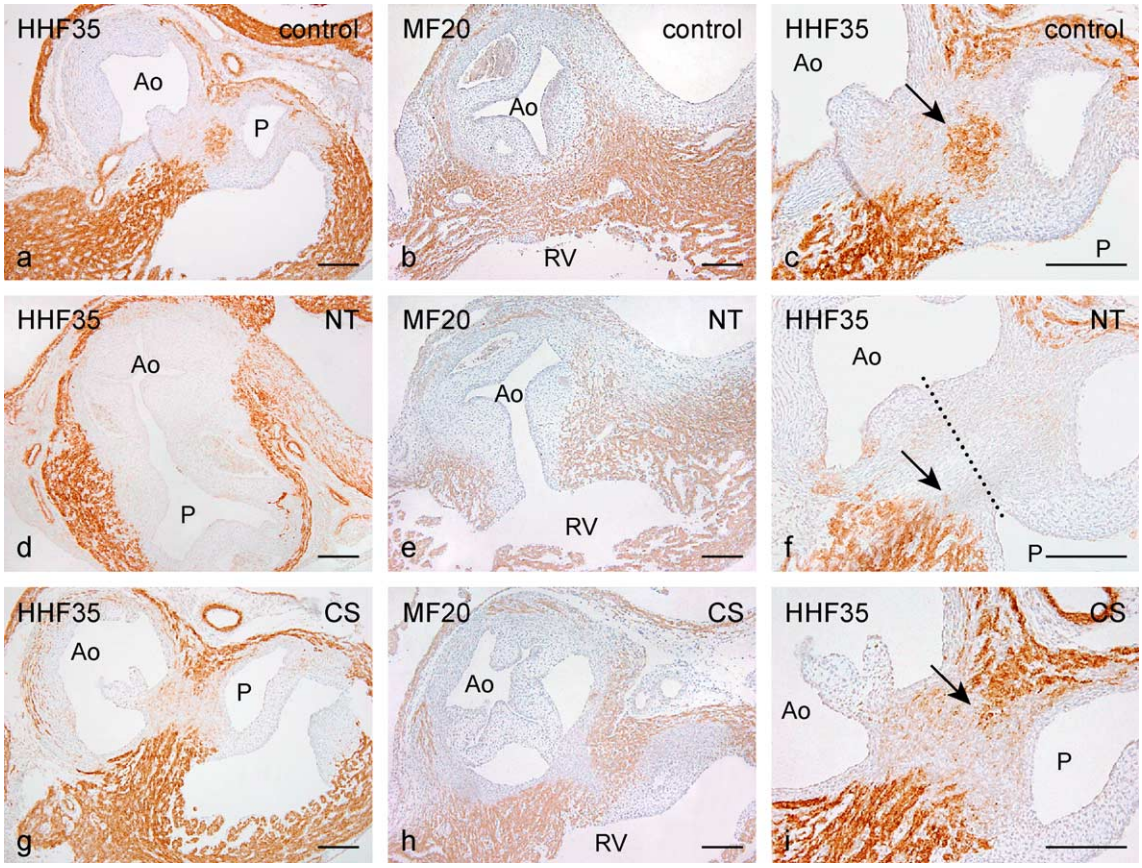


Fig. 4. Transverse sections of the outflow tract of HH35 embryos. (a–c) Control embryos. (a) The aortic and pulmonary valves are separated by mesenchyme invaded by myocardial cells. (b) Myosin heavy chain staining (MF-20) at a lower level shows the myocardialized cushion tissue separating the aorta from the right ventricular outflow tract. (c) Detail of panel (a) showing the tip of the myocardialized septum (arrow). (d–f) NT embryos. (d) Outflow tract cushions have failed to fuse, resulting in a subarterial VSD and almost absent myocardialization. (e) The subarterial VSD involves the aortic valve and the right ventricular outflow tract. (f) Septum between aortic and pulmonary valves displays reduced myocardial cell invasion (arrow), dotted line indicates the position of the subarterial VSD approximately 30 μm below this section. (g–i) CS embryos. (g) Outflow cushions have fused and myocardialization has taken place. (h) Area in between aortic valve and right ventricular outflow tract is almost completely invaded by myocardial cells. (i) Detail of panel (g) showing myocardial cell invasion into the central area between the pulmonary and aortic valves (arrow). Ao, aorta; P, pulmonary trunk; RV, right ventricular outflow tract; NT, homocysteine-neural tube injected; CS, homocysteine-circulatory system injected. Bar=150 μm.

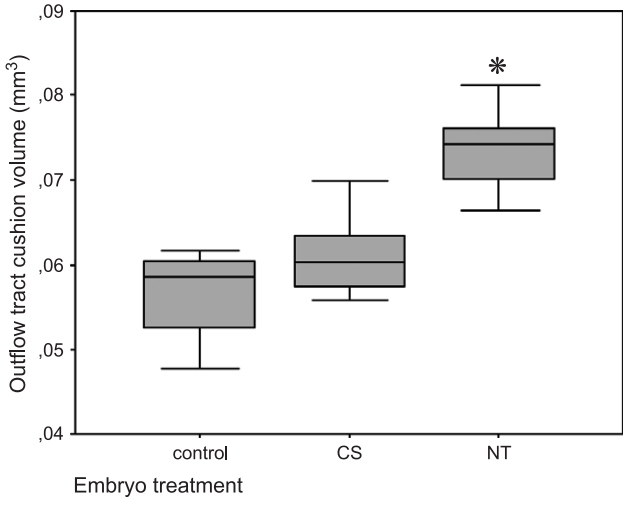


Fig. 5. Outflow tract cushion volume in control embryos, CS embryos, and NT embryos. The volume of outflow tract cushion tissue is 25% larger in NT than in control embryos, this is significant ($p<0.005$) as demonstrated with the Mann–Whitney test. *$p<0.005$.

Out of the five NT embryos with a subarterial VSDs, only one embryo displayed an abnormal pharyngeal arch artery system. This embryo showed complete absence of both left and right fourth pharyngeal arch arteries. However, endothelial cell detachment and abnormal extracellular matrix deposition were observed in the pharyngeal arch arteries [21].

A three-dimensional reconstruction was generated to analyze the anatomical relations of the lumen of the ascending aorta, pulmonary trunk, left ventricle and right ventricle of a control (Fig. 6a) and an NT embryo (Fig. 6c). The reconstruction of the latter clearly demonstrates the high subarterial VSD. Although the reconstruction shows that the position of the pulmonary trunk in relation to the aorta is slightly deviant, the aorta is not positioned above the right ventricle as in a double outlet right ventricle.

The reconstructions of the lumen of the ascending aorta and the pulmonary trunk, together with the outflow tract cushion tissue of a control embryo (Fig. 6b) and a NT embryo (Fig. 6d) demonstrate that in the NT embryo

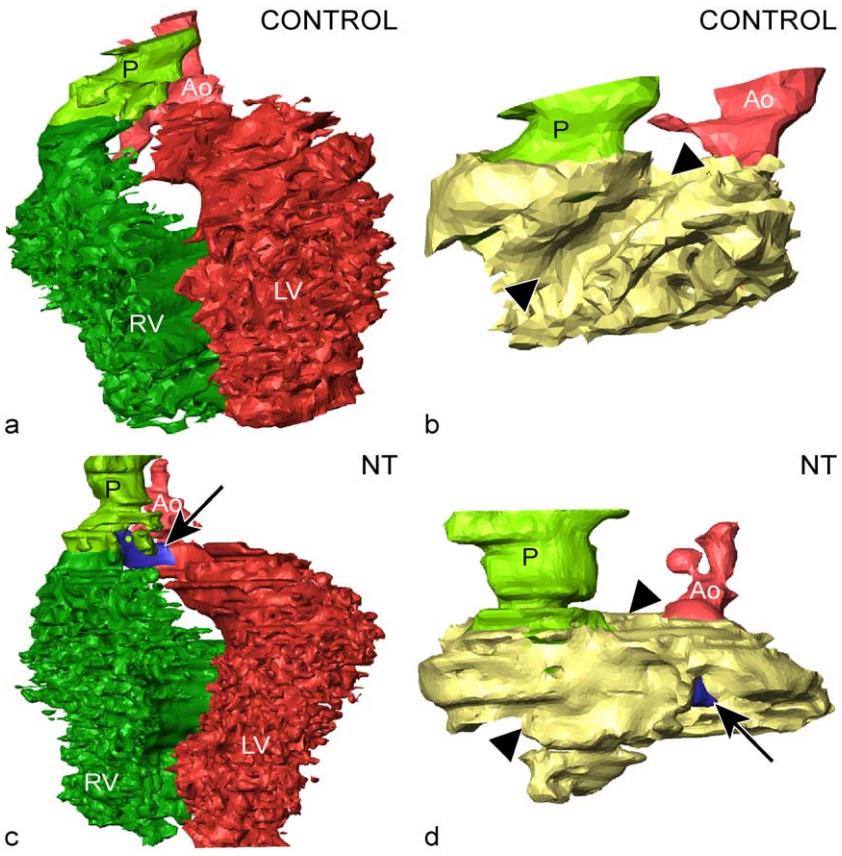


Fig. 6. Three-dimensional reconstructions of HH35 embryos. (a–b) Control embryo. (a) Lumen of ascending aorta, pulmonary trunk, left and right ventricles are shown. (b) Lumen of ascending aorta and pulmonary trunk, together with the outflow tract cushion tissue. Note that the central area of the cushion is concave (between arrowheads), this is due to myocardialization of the outflow cushions. (c–d) NT embryo. (c) Lumen of ascending aorta, pulmonary trunk, left and right ventricle are shown, together with a high, subarterial VSD indicated in blue (arrow). (d) Lumen of the ascending aorta and pulmonary trunk, a small part of the subarterial VSD (arrow) positioned in the outflow tract cushion tissue. Note that the central area of the outflow tract cushion tissue is bulging, because of lack of myocardialization (between arrowheads).

the outflow tract cushion tissue is bulging in the central area between the left and right outflow tract, compared to the concave central area in the control embryos. This is the area where myocardialization has taken place in the outflow cushions of the control embryos, but not in NT embryos.

## 4. Discussion

After exposure to homocysteine we observed no changes in *Pax3* expression in the neural tube, nor in the mesenchyme surrounding the neural tube. Previous studies showed that folic acid is able to prevent neural tube defects in the *Pax3* deficient *Splotch* mouse model [17]. Our results do not show a relation between *Pax3* and homocysteine, this might suggest that the prevention of neural tube defects in *Pax3* deficient mice are not associated with the homocysteine-lowering effects of folic acid.

In vitro studies demonstrated increased neural crest cell migration rates in the presence of homocysteine [15]. In the current study we traced *lacZ*-positive cardiac neural crest cells on their pathway to the outflow tract of the heart and observed no differences in timing between control and NT embryos when cardiac neural crest cells arrive at the aortic sac. This suggests that the differences in migration rate are either too small to observe, or that there is no effect of homocysteine on migration rate in vivo.

We postulated in a previous study that cardiac neural crest cells play an important role in myocardialization of the outflow tract, while neural crest cells exhibit exceptional high levels of apoptosis at the stage when cardiomyocytes muscularize the outflow tract [13]. Outflow tract myocardialization [26] is a process that is regulated by gene cascades that are largely unknown. Members of the Tgfβ family have been suggested to play a role in this process. In Tgfβ-2 knockout mouse embryos, incomplete myocardialization of the outflow tract septum is observed [27] and the expression pattern of Tgfβ-2 during embryonic development suggests a function in the process of myocardialization [28].

Poelmann et al. [29] hypothesized that neural crest apoptosis might activate myocardialization through activation of matrix bound Tgf-β. In the current study, we

demonstrate that *lacZ*-positive cardiac neural crest cells reach the pharyngeal arch arteries, the aorticopulmonary septum and outflow tract cushions in both control and NT embryos. However, at HH31 the myocardialization of the outflow tract cushions is less, and the number of TUNEL-positive apoptotic cells is 60% lower in NT embryos.

We hypothesize that after exposure to homocysteine, the neural crest cells migrate to the outflow tract, display a different gene expression pattern, and fail to undergo apoptosis and as a consequence are unable to provide the signals required for myocardialization of the outflow tract. This complies with the significant 25% larger volume of outflow tract cushion tissue that had not been myocardialized in NT embryos. In addition to the neural crest cells also cardiomyocytes undergo apoptosis in the myocardialization area of the outflow tract. Signals to induce cardiomyocyte apoptosis seem to originate from the epicardium [30]. This suggests that the complex remodeling of the outflow tract and myocardialization is dependent on intense apoptosis of both neural crest cells and cardiomyocytes.

The incidence of subarterial VSD in the NT embryos at HH35 is very high (83%, 5 out of 6 embryos). Different results were obtained in a study [9] with chick embryos that received a solution of homocysteine (100 mmol/l, namely 5 μmol in 50 μl) on the inner embryonic membrane for three consecutive days: only 22% (4 out of 18 embryos) showed a VSD, while a high percentage (79%) displayed a ventral midline closure defect. The high incidence of outflow tract malformations that we observed is probably due to the specific application of homocysteine to the premigratory neural crest in our model. In addition, the 30 μmol/l dose used in our study is much lower than the dose used by Rosenquist et al. [9] and is comparable to the mildly elevated fasting homocysteine concentrations (19–27 μmol/l) as described in blood plasma in a subset of mothers of offspring with a neural tube defect [31].

Interestingly, we demonstrated in this study that the CS embryos do not display subarterial VSDs or reduced myocardialization of the outflow tract cushions. It is conceivable that the CS embryos which received 30 μmol/l homocysteine might not have resulted in subarterial VSDs due to the dilution of the homocysteine solution (approximately 8 times) into the blood volume of the embryo. However, even the 10-fold higher homocysteine solution (300 μmol/l) did not result in subarterial VSD formation. The subarterial VSDs and reduced myocardialization in homocysteine-neural tube injected embryos might, therefore, be explained by a specific effect of homocysteine on neural crest cells.

The present study suggests a relation between homocysteine, neural crest cell behavior, and the development of subarterial VSDs in chick embryos.

Hyperhomocysteinemia with an estimated prevalence of 1:70 in the human population [32] is not a rare phenomenon. This means large numbers of pregnant women will expose their yet unborn offspring to hyperhomocysteinemic concentrations. Future research is necessary to address what the impact is of homocysteine on heart development in fetuses of hyperhomocysteinemic women.

## Acknowledgements

We thank Jan Lens for the photographic contributions, Bert Wisse for 3D Amira reconstructions (Dept. of Anatomy and Embryology, LUMC), and Jano van Hemert (Center for Mathematics and Computer Science, Amsterdam) for assistance with the statistical analysis.

## References

[1] Botto LD, Moore CA, Khoury MJ, Erickson JD. Neural-tube defects. N Engl J Med 1999;341:1509–19.
[2] MRC Vitamin Study Research Group. Prevention of neural tube defects: results of the Medical Research Council Vitamin Study. Lancet 1991;338:131–7.
[3] Shaw GM, O'Malley CD, Wasserman CR, Tolarova MM, Lammer EJ. Maternal periconceptional use of multivitamins and reduced risk for conotruncal heart defects and limb deficiencies among offspring. Am J Med Genet 1995;59:536–45.
[4] Botto LD, Khoury MJ, Mulinare J, Erickson JD. Periconceptional multivitamin use and the occurrence of conotruncal heart defects: results from a population-based, case-control study. Pediatrics 1996;98:911–7.
[5] Kang SS, Wong PW, Norusis M. Homocysteinemia due to folate deficiency. Metabolism 1987;36:458–62.
[6] Steegers-Theunissen RP, Boers GH, Trijbels FJ, Eskes TK. Neural-tube defects and derangement of homocysteine metabolism. N Engl J Med 1991;324:199–200.
[7] Steegers-Theunissen RP, Boers GH, Blom HJ, et al. Neural tube defects and elevated homocysteine levels in amniotic fluid. Am J Obstet Gynecol 1995;172:1436–41.
[8] Kapusta L, Haagmans ML, Steegers EA, Cuypers MH, Blom HJ, Eskes TK. Congenital heart defects and maternal derangement of homocysteine metabolism. J Pediatr 1999;135:773–4.
[9] Rosenquist TH, Ratashak SA, Selhub J. Homocysteine induces congenital defects of the heart and neural tube: effect of folic acid. Proc Natl Acad Sci U S A 1996;93:15227–32.
[10] Kirby ML, Turnage KL, Hays BM. Characterization of conotruncal malformations following ablation of "cardiac" neural crest. Anat Rec 1985;213:87–93.
[11] Le Lièvre CS, Le Douarin NM. Mesenchymal derivatives of the neural crest: analysis of chimaeric quail and chick embryos. J Embryol Exp Morphol 1975;34:125–54.
[12] Verberne ME, Gittenberger-de Groot AC, Van Iperen L, Poelmann RE. Distribution of different regions of cardiac neural crest in the extrinsic and the intrinsic cardiac nervous system. Dev Dyn 2000;217:191–204.
[13] Poelmann RE, Mikawa T, Gittenberger-de Groot AC. Neural crest cells in outflow tract septation of the embryonic chicken heart: differentiation and apoptosis. Dev Dyn 1998;212:373–84.
[14] Boot MJ, Gittenberger-de Groot AC, van Iperen L, Hierck BP, Poelmann RE. Spatiotemporally separated cardiac neural crest subpopulations that target the outflow tract septum and pharyngeal arch arteries. Anat Rec 2003;275A:1009–18.
[15] Brauer PR, Rosenquist TH. Effect of elevated homocysteine on cardiac neural crest migration in vitro. Dev Dyn 2002;224:222–30.
[16] Boot MJ, Steegers-Theunissen RP, Poelmann RE, van Iperen L, Lindemans J, Gittenberger-de Groot AC. Folic acid and homocysteine

affect neural crest and neuroepithelial cell outgrowth and differentiation in vitro. Dev Dyn 2003;227:301–8.
[17] Fleming A, Copp AJ. Embryonic folate metabolism and mouse neural tube defects. Science 1998;280:2107–9.
[18] Hamburger V, Hamilton HL. A series of normal stages in the development of the chick embryo. J Morphol 1951;88:49–92.
[19] Mikawa T, Fischman DA, Dougherty JP, Brown AMC. In vivo analysis of a new lacZ retrovirus vector suitable for cell lineage marking in avian and other species. Exp Cell Res 1991;195:516–23.
[20] Boot MJ, Gittenberger-de Groot AC, van Iperen L, Poelmann RE. The myth of ventrally emigrating neural tube (VENT) cells and their contribution to the developing cardiovascular system. Anat Embryol 2003;206:327–33.
[21] Boot MJ, Steegers-Theunissen RP, Poelmann RE, van Iperen L, Gittenberger-de Groot AC. Homocysteine induces endothelial cell detachment and vessel wall thickening during chick embryonic development. Circ Res 2004;94(4):542–9.
[22] Molin DGM, DeRuiter MC, Wisse LJ, et al. Altered apoptosis pattern during pharyngeal arch artery remodelling is associated with aortic arch malformations in Tgf beta 2 knock-out mice. Cardiovasc Res 2002;56:312–22.
[23] Moorman AF, Houweling AC, de Boer PA, Christoffels VM. Sensitive nonradioactive detection of mRNA in tissue sections: novel application of the whole-mount in situ hybridization protocol. J Histochem Cytochem 2001;49:1–8.
[24] Gundersen HJG, Bendtsen TF, Korbo L, et al. Some new, simple and efficient stereological methods and their use in pathological research and diagnosis. APMIS 1988;96:379–94.
[25] Bouman HGA, Broekhuizen MLA, Baasten AMJ, Gittenberger-de Groot AC, Wenink ACG. Stereological study of stage 34 chicken hearts with looping disturbances after retinoic acid treatment: disturbed growth of myocardium and atrioventricular cushion tissue. Anat Rec 1997;248:242–50.
[26] van den Hoff MJ, Moorman AF, Ruijter JM, et al. Myocardialization of the cardiac outflow tract. Dev Biol 1999;212:477–90.
[27] Bartram U, Molin DGM, Wisse LJ, et al. Double-outlet right ventricle and overriding tricuspid valve reflect disturbances of looping, myocardialization, endocardial cushion differentiation, and apoptosis in TGFß2-knockout mice. Circulation 2001;103:2745–52.
[28] Molin DG, Bartram U, Van der Heiden K, et al. Expression patterns of Tgfbeta1-3 associate with myocardialisation of the outflow tract and the development of the epicardium and the fibrous heart skeleton. Dev Dyn 2003;227(3):431–44.
[29] Poelmann RE, Molin D, Wisse LJ, Gittenberger-de Groot AC. Apoptosis in cardiac development. Cell Tissue Res 2000;301:43–52.
[30] Rothenberg F, Hitomi M, Fisher SA, Watanabe M. Initiation of apoptosis in the developing avian outflow tract myocardium. Dev Dyn 2002;223:469–82.
[31] Steegers-Theunissen RP, Boers GH, Trijbels FJ. Maternal hyperhomocysteinemia: a risk factor for neural-tube defects? Metabolism 1994;43:1475–80.
[32] Loscalzo J. The oxidant stress of hyperhomocyst(e)inemia. J Clin Invest 1996;98:5–7.